Comparative analysis of SAR sensors for effective tectonic lineament mapping in semi-arid region

Mohcine Chakouri[1*], *Amine* Jellouli[1], *Soufiane* Hajaj[1], *Jaouad* EL Hachimi[1], *Abdelkarim* Ouguinaz[2], *Abdelhaq* Aangri[3,4] and *Abderrazak El Harti[1]*

[1] Team of Remote Sensing and GIS, Faculty of Sciences and Techniques, PO BOX 523, Beni Mellal, Morocco.
[2] Research Group on Geography and Development, Faculty of Arts and Humanities, Abdelmalek Saadi University; Morocco.
[3] Natural Resources and Sustainable Development Laboratory, Geosciences and Environment Team, Faculty of Science, Ibn Tofail University, Kenitra, Morocco.
[4] SHOM (DOPS/STM/REC), Toulouse, France.

Abstract. The progression and refinement of remote sensing techniques now allow the extraction of geological lineaments without traditional methods. This study aims to detect lineaments using Synthetic Aperture Radar (SAR) data from three sensors with different bands: Alos-Palsar, Radarsat-1, and Sentinel-1. Automatic lineament extraction is performed by combining two different parameters along with the Palsar Digital Elevation Model in order to recommend the most powerful sensor for this task. The methodology involves relating the length, number, orientation, and density of lineaments to surface features such as slope, lithology, and discontinuities. The results of this evaluation show that the lineaments obtained of both polarizations of sentinel correlate better with geological units, the orientation of the tectonic system, shadow and slope maps. This is attributable to the high efficiency of VH polarization, which is not dependent on soil characteristics, in comparison with other polarizations that overestimated lineaments with different directions.

Keywords: Lineament extraction; Remote sensing; Radar; Digital Elevation Model.

1 Introduction

Structural geology is crucial for any petroleum, geotechnical, or mineral exploration. Geological mapping relies on understanding structures like faults, fractures, folds, and breaks, and lineament mapping is essential for identifying these structures [1-4]. Therefore, any geological mapping study requires background of structural information, including faults, fractures, folds and brittle features. Lineament mapping is essential for identifying these structural details.

* Corresponding author: chakouri.mohcine@gmail.com

[5] defines lineaments as linear or curved features related to geological structures. Their presence often indicates mining potential. Remote sensing, particularly, facilitates the extraction of lineaments from various data, though manual mapping is difficult and time-consuming.

Optical remote sensing is widely used to map lineaments using multi and hyperspectral image data. [3, 6]. Studies show that both optical and SAR data are highly suitable for this task. [7], although SAR data is less used despite its ability to provide measurements under all weather conditions and at any time.

Launched in 1995, RADARSAT-1 is an Earth observation satellite developed by the Canadian Space Agency. It operates in C-band with a 10-meter resolution and covers a 50 km² area in fine beam mode, The related data are valuable in various areas, including ocean monitoring [8], Forestry [9], and geology [10].

Launched in 2014 by the ESA, Sentinel-1 provides C-band SAR images with a 5x20 meter resolution and incidence angles from 31° to 46° [11]. Sentinel-1 data is free and useful in various fields [12].

The PALSAR radar on ALOS, launched in 2006 by JAXA, uses the L-band and has captured 2.10 million imageries in HH and VV polarization, with angles of incidence from 18° to 43°. These data are invaluable for environmental protection and exploration. [13, 14].

ALOS also provides high and low-resolution DEMs, useful for lineament extraction. This research compares the performance of RADARSAT-1, Sentinel-1, and ALOS PALSAR data for automatic lineament detection in a semi-arid region.

2 Geographic and Geological Characteristics of the Study Area:

The massif of Jebilet, situated at latitudes 31° 40' N and 32° N with longitudes 8° 20' W and 7° 40' W, is approximately 10 km to the north of the city of Marrakech. (**Fig.1**). The site was selected for its geological diversity, its mineral resources and the in-depth geological investigations that have already been carried out in the study area [15-18].

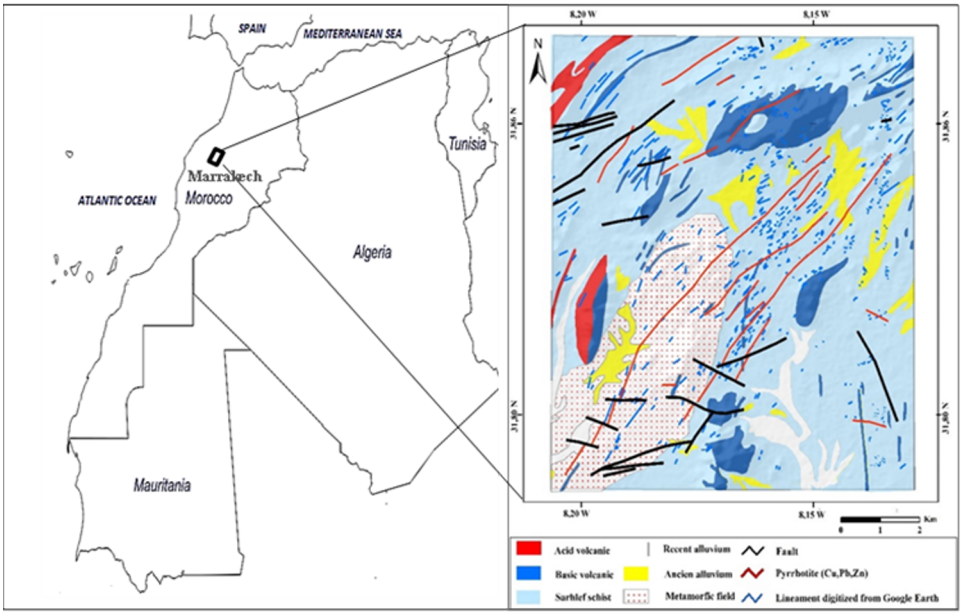

Fig. 1. National scale map of our area of interest (left), and 1:100,000 scaled geology and mineralogy map of the Central Jebilet (right).

3 Materials and Methods

3.1 Dataset

The radar data covering our study area include:
One Radarsat-1 scene from October 13, 1997, in C-band Standard mode with HH polarization, two Sentinel-1A images from October 18, 2017, in C-band Interferometric Wide with two polarizations, two Alos Palsar scenes from June 14, 2007, in L-band Fine Beam mode with HH and HV polarizations and a DEM of 12-meter resolution.

3.2 Methodology

3.2.1 Preprocessing steps

Prior to using satellite images, essential pre-processing steps are undertaken. This phase converts digital numbers (DN) into backscatter values and reduces atmospheric effects like "salt and pepper" noise (speckle) using the Lee filter across SAR images from three sensors. Geometric correction follows to rectify distortions caused by terrain relief and sensor tilt [19], employing Alos Palsar's high-precision (12m) Digital Elevation Model (DEM) with SNAP tools and the Range Doppler Orthorectification method.

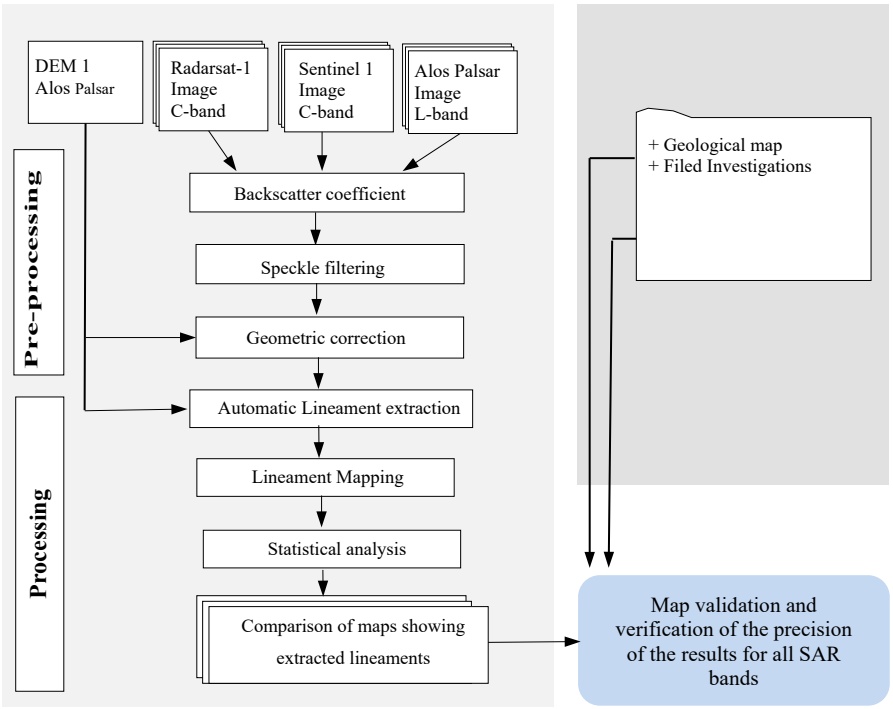

Fig. 2. Flowchart of this work

3.2.2 Processing

In this work, extracting the lineament was automated using two main methods:

Contour Detection: Implemented a Gaussian filter (RADI parameter) to detect abrupt changes in pixel values, crucial for locating lineaments. A binary edge image was then generated using the Edge Gradient Threshold (GTHR).
Line Extraction: Utilized the PCI Geomatica software's Line module, validated for its ability to extract lineaments using six key parameters: RADI (Filter radius), GTHR (Edge Gradient Threshold), LTHR (Length threshold), FTHR (Line Fitting Threshold), ATHR (Angular Difference Threshold), and DTHR (Linking Distance Threshold). Additionally, the study considered:
Slope: Important for identifying lineaments based on changes in DEM slope.
Shaded Relief: Used grayscale images to detect lineaments by analyzing shadow patterns based on sun position, with the north-south orientation proving most effective. This methodology optimized the Line module's performance in accurately identifying and mapping lineaments across the study area.

4 Results and Discussion

Statistical analysis of the results shows in (**Fig. 3**) that 706 lineaments were detected from Palsar HH images, 545 from HV images, and 684 from Radarsat-1 HH polarization. Additionally, Sentinel-1's both polarizations contributed 230 and 255 lineaments, respectively. Regarding measurement of lineament lengths, those extracted from Palsar HH polarization range from 128m to 1604m, and from HV polarization from 128m to 1200m. Lineaments derived from Radarsat-1 data vary between 137m and 1403m, while those from Sentinel-1's two polarization span from 170m to 3134m and 170m to 3038m, respectively.

This difference in lineament lengths can be attributed to polarization characteristics. Lineaments from horizontally polarized data tend to have shorter minimum lengths compared to those from vertically polarized data, while the opposite holds true for longer lengths (Sentinel-1 image exhibit significantly longer maximum lineament lengths compared to Palsar and Radarsat-1 data). The majority of lineaments from Palsar HH and HV data range between 128m and 280m, while for Radarsat-1 data, the most common lengths fall between 137m and 360m. Sentinel-1 VH and VV data show predominant lengths between 170m and 340m.

To assess sensor efficiency in detecting abrupt changes and slope areas, the lineaments obtained from the RADAR sensors have been superimposed on the slope mapping (**Fig. 5**). Analysis revealed that lineaments from Sentinel-1's both polarizations aligned well with slope, particularly over areas of acid and basic volcanic units, where significant altitude changes occur in the study area. contrary, lineaments from both polarizations of Palsar were located across most slope areas, including those with consistent slope. Regarding Radarsat-1 HH polarization data, lineament distribution showed no clear correlation with slope parameters, except for those well-represented in the northeastern part of the study area across all SAR images.

It is essential to assess lineament results by examining their orientation relative to ground truth. **(Fig.4)** shows a rose diagram illustrating the orientations of various elements including lineaments extracted from SAR data sources: (a) HH, (b) HV polarizations of Alos Palsar, (c) HH polarization of Radarsat-1, (d) VH polarization, and (e) VV polarization of Sentinel-1. The HH lineaments obtained from polarization of Palsar exhibit diverse orientations (**Fig. 4a**), while those from HV polarization (**Fig 4b**) predominantly align along the northeast-southwest direction (NE 45, SW 225), with other directions also present. Similarly, Radarsat-1 HH data follow the northeast-southwest direction (NE 45, SW 225) (**Fig 4c**). Sentinel-1 data clearly show a predominant northeast-southwest orientation, with VH (**Fig. 4 d**) at NE 45, SW 235 and VV (**Fig. 4e**) at NE 45, SW 225. The orientations of faults (**Fig. 4f**), digitized lineaments (**Fig. 4g**), and veins of Zn, Cu (**Fig. 4h**) correlate closely with the northeast-

southwest directions observed in Sentinel-1 images (NE 75, SW 260 for faults; NE 55, SW 235 for digitized lineaments; NE 45, SW 225 for Hercynian veins).

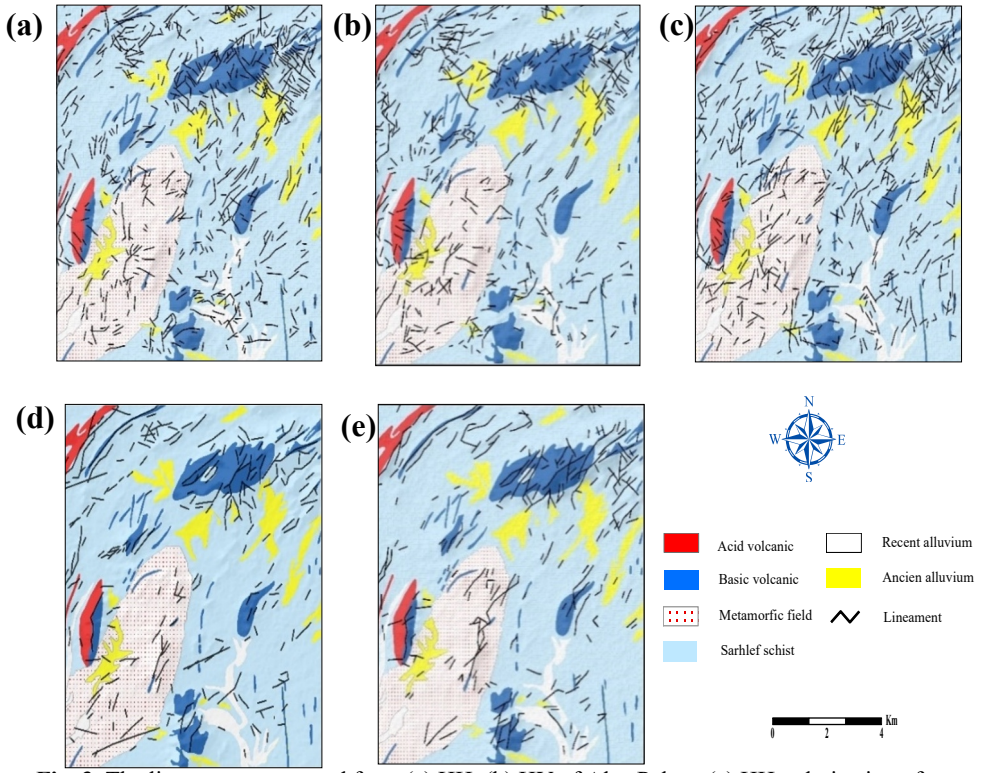

Fig. 3. The lineaments extracted from (a) HH, (b) HV of Alos Palsar, (c) HH polarization of Radarsat-1, and (d) VH (e) VV of Sentinel-1 have been overlaid onto the digitalized geological map.

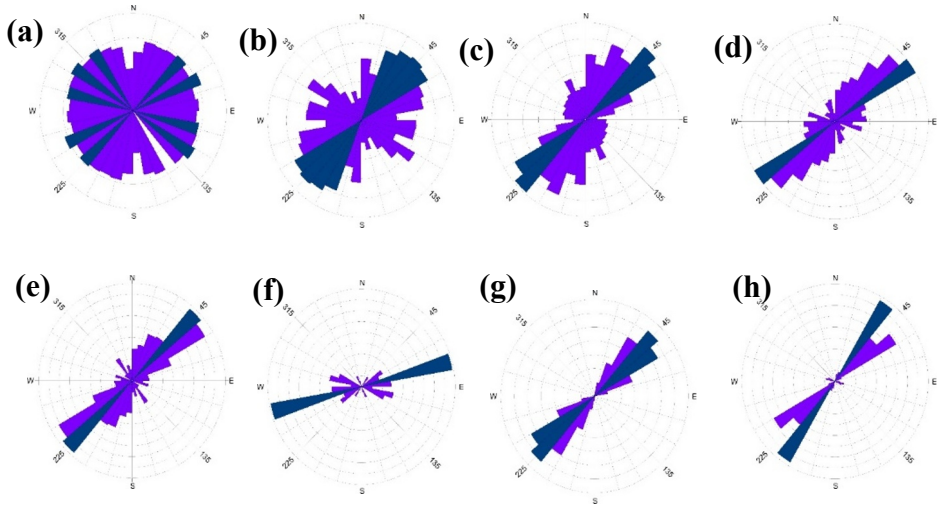

Fig.4. The Rose diagrams display the directions of various lineaments extracted from SAR data sources: (a) HH , (b) HVof Alos Palsar, (c) HH of Radarsat-1, (d) VH (e) VV Sentinel-1, along with (f) digitized lineaments from Google Earth, (g) faults, and (h) Veins of Zn, Cu.

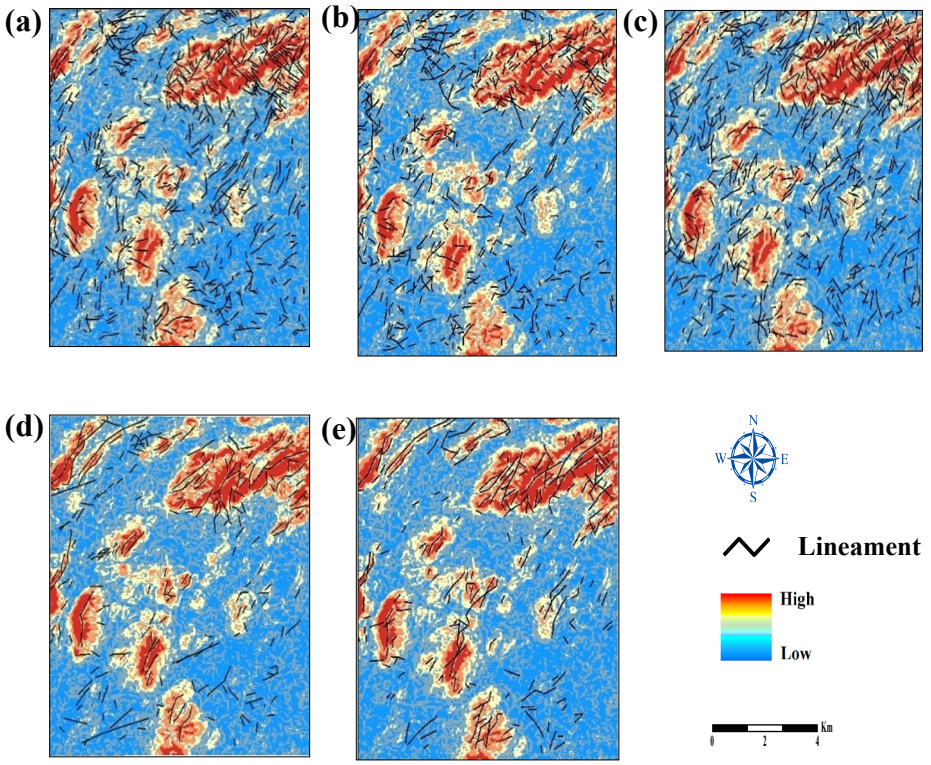

Fig. 5. The lineaments extracted from (a) HH and (b) HV polarizations of Alos Palsar, (c) HH polarization of Radarsat-1, and (d) VH and (e) VV polarizations of Sentinel-1 have been overlaid onto the slope map

5 Conclusion:

This work aims to evaluate the performance of the automatic detection from three different sensors in identifying lineaments. The analysis compared data obtained from these sensors, considering slope, shading, and orientation parameters. Validation was conducted using geological maps and field investigations, correlating lithological units with extracted lineament locations. Sentinel-1, particularly VH polarization data, demonstrated superior performance in automatic lineament mapping compared to other sensors, which showed less correlation with the studied parameters. Our findings were validated by mining exploration experts from a major international company operating in the study area's existing mines.

Funding
the authors declare that they have not received any financial support for this research work and that this article is not an issue of conflict of interest.

Author contribution
The authors (A. Aangri, A. Ouguinaz and A. El Harti) validated the document and worked on the design, (A.Jellouli, S. Hajjaj and J. El Hachimi contributed to the methodology, (M Chakouri) reviewed and grouped the ideas and wrote the text of the manuscript.

Ethics approval and consent to participate
Not applicable.
Consent to publication
All authors give permission for publication.
Competing interests
All the authors declare that they don't have no competing of interests.
Acknowledgement
We would like to thank the European Space Agency for giving us access to Sentinel data, and the Canadian Space Agency for providing us with free RADARSAT data.

References

[1] E. Farahbakhsh, R. Chandra, H. K. Olierook, R. Scalzo, C. Clark, S. M. Reddy, et al., Computer vision-based framework for extracting tectonic lineaments from optical remote sensing data. International Journal of Remote Sensing. 41,1760-1787, (2020).

[2] A. Javhar, X. Chen, A. Bao, A. Jamshed, M. Yunus, A. Jovid, et al., Comparison of multi-resolution optical Landsat-8, Sentinel-2 and radar Sentinel-1 data for automatic lineament extraction: a case study of Alichur Area, SE Pamir. Remote Sensing. 11,778, (2019).

[3] A. Jellouli, A. El Harti, Z. Adiri, M. Chakouri, J. El Hachimi, and E. M. Bachaoui, Application of optical and radar satellite images for mapping tectonic lineaments in kerdous inlier of the Anti-Atlas belt, Morocco. Remote Sensing Applications: Society and Environment. 22,100509, (2021).

[4] A. Shebl and Á. Csámer, Reappraisal of DEMs, Radar and optical datasets in lineaments extraction with emphasis on the spatial context. Remote Sensing Applications: Society and Environment. 24,100617, (2021).

[5] M. Heddi, D. Eastaff, and J. Petch, Relationships between tectonic and geomorphological linear features in the Guadix-Baza basin, southern Spain. Earth Surface Processes and Landforms. 24, 931-942, (1999).

[6] S. Hajaj, A. El Harti, and A. Jellouli, Assessment of hyperspectral, multispectral, radar, and digital elevation model data in structural lineaments mapping: A case study from Ameln valley shear zone, Western Anti-Atlas Morocco. Remote Sensing Applications: Society and Environment. 27,100819, 2022.

[7] M. Mwaniki, D. N. Kuria, M. Boitt, and T. Ngigi, Image enhancements of Landsat 8 (OLI) and SAR data for preliminary landslide identification and mapping applied to the central region of Kenya. Geomorphology, 282, 162-175, (2017).

[8] K. Ouchi, Synthetic Aperture Radar Over Ocean: A Review, IEICE Technical Report; IEICE Tech. Rep. 121, 1-6, (2021).

[9] S. Cote, M. Lapointe, P.-P. Vezina, E. Arsenault, C. Casgrain, and A. Boyer, Status of the RADARSAT Constellation Mission in the third year of operation, in EUSAR. 14th European Conference on Synthetic Aperture Radar. 1-6, (2022).

[10] S. G. Ouattara, B. Dibi, and J. M. O. Mangoua, Contribution of RADARSAT-1 Images to Structural Geological Mapping and Lineament Density Assessment in the Lobo River Watershed at Nibéhibé (Centre-West, Côte d'Ivoire). European Journal of Environment and Earth Sciences, 2,15-20, (2021).

[11] R. Torres, P. Snoeij, D. Geudtner, D. Bibb, M. Davidson, E. Attema, et al., GMES Sentinel-1 mission. Remote Sensing of Environment,120, 9-24, (2012).

[12] S. Mastrorosa, M. Crespi, L. Congedo, and M. Munafò, Land Consumption Classification Using Sentinel 1 Data: A Systematic Review. Land, 12, p. 932, (2023).

[13] A. B. Pour, B. Zoheir, B. Pradhan, and M. Hashim, Editorial for the special issue: Multispectral and hyperspectral remote sensing data for mineral exploration and environmental monitoring of mined areas.13, 519, (2021).
[14] L. San Martín, N. S. Morandeira, R. Grimson, M. Rajngewerc, E. B. González, and P. Kandus, The contribution of ALOS/PALSAR-1 multi-temporal data to map permanently and temporarily flooded coastal wetlands. International Journal of Remote Sensing, 41,1582-1602, (2020).
[15] A. Aboulfaraj, A. Tabit, A. Algouti, A. Algouti, S. Moujane, A. Farah, et al., Contribution of Remote Sensing and Structural Geology in the Mapping of Tectonic Fractures in the Zat Region (Western High Atlas, Morocco). Journal of the Indian Society of Remote Sensing, 1-21, (2024).
[16] P. Huvelin, Etude géologique et gîtologique du massif hercynien des Jebilet (Maroc occidental): Service géologique du Maroc, (1977).
[17] M. Chakouri, R. Lhissou, A. El Harti, S. Maimouni, and Z. Adiri, Assessment of the image-based atmospheric correction of multispectral satellite images for geological mapping in arid and semi-arid regions. Remote Sensing Applications: Society and Environment, 20,100420, (2020).
[18] M. Chakouri, A. El Harti, R. Lhissou, J. El Hachimi, and A. Jellouli, Geological and mineralogical mapping in Moroccan central Jebilet using multispectral and hyperspectral satellite data and machine learning. Int. J, 9, 5772-5783, (2020).
[19] J. Cheng, Q. Xiao, J. Wen, Y. Tang, D. You, Z. Bian, et al., Review of methods and remote sensing cases using spectral library. Remote Sensing Technology and Application, **35**, 267-286, (2020).